Observational evidence of the generation mechanism for rising-tone chorus

C. M. Cully,[1] V. Angelopoulos,[2] U. Auster,[3] J. Bonnell,[4] and O. Le Contel[5]

Received 8 October 2010; revised 9 November 2010; accepted 15 November 2010; published 13 January 2011.

[1] Chorus emissions are a striking feature of the electromagnetic wave environment in the Earth's magnetosphere. These bursts of whistler-mode waves exhibit characteristic frequency sweeps (chirps) believed to result from wave-particle trapping of cyclotron-resonant particles. Based on the theory of Omura et al. (2008), we predict the sweep rates of chorus elements observed by the THEMIS satellites. The predictions use independent observations of the electron distribution functions and have no free parameters. The predicted chirp rates are a function of wave amplitude, and this relation is clearly observed. The predictive success of the theory lends strong support to its underlying physical mechanism: cyclotron-resonant wave-particle trapping.
Citation: Cully, C. M., V. Angelopoulos, U. Auster, J. Bonnell, and O. Le Contel (2011), Observational evidence of the generation mechanism for rising-tone chorus, *Geophys. Res. Lett.*, *38*, L01106, doi:10.1029/2010GL045793.

1. Introduction

[2] Chorus emissions are whistler-mode waves generated in-situ in the Earth's magnetosphere. They derive their name from their identifying characteristic: short chirps of rising (typical) and/or falling (less common) tones in the audio range. The electron distributions in regions where chorus is present are often anisotropic, with $T_\perp > T_{||}$ [*Tsurutani et al.*, 1979; *Li et al.*, 2010], and whistler-mode waves are expected based on linear theory [*Helliwell*, 1965; *Kennel and Petschek*, 1966]. However, the linear theory fails to explain the characteristic chirping. These emissions offer a clear example of how nonlinear effects can lead to qualitatively different behavior in a physical system.

[3] The shortcomings of the linear theory drove attention to nonlinear theories, where it was first shown that whistler waves in an inhomogeneous medium could stably trap cyclotron-resonant electrons [*Dysthe*, 1971], and that the resonant current thereby produced could lead to strong wave amplification [*Nunn*, 1974; *Omura et al.*, 1991; *Trakhtengerts*, 1999]. Starting from the incoherent hiss predicted by linear theory, cyclotron-resonant electrons become trapped in the wave field, leading to strong nonlinear amplification and chirping.

[4] Although the cyclotron-resonant trapping theory is well developed, it is difficult to test directly. The essential feature of the theory is the alteration of the distribution function through phase-bunching of electrons, which has been demonstrated in electron-hybrid simulations by *Katoh and Omura* [2007], who term the resulting structure in phase space an "electromagnetic electron hole". Unfortunately, the electromagnetic electron hole rotates with the local gyrofrequency (order of kHz) making its direct observation impossible with any existing electron instrument.

[5] Although observing the electron hole itself is not practical, there are other ways of experimentally testing the available theories; *Santolík* [2008] provides a good review. Using a Vlasov hybrid simulation, *Nunn et al.* [2009] were able to successfully reproduce chorus elements similar to those observed by the Cluster satellites, while *Trakhtengerts et al.* [2007] and *Santolík et al.* [2008] were able to explain the spatial variation of observed chorus frequency.

[6] Recently, *Omura et al.* [2008, hereafter OKS08] pointed out another possible test: their theory predicts a sweep rate that is a function of wave amplitude. The theory applies to narrowband, rising-tone chorus, excluding both the (rare) falling tones [*Tsurutani and Smith*, 1974], and fine amplitude structures within the packet [*Santolík et al.*, 2004]. They showed agreement with simulations and pointed out a rough consistency with published observations. In this paper, we follow up on this proposed amplitude-sweep rate relation by first extending OKS08's relation to use arbitrary distribution functions, and then directly comparing the resulting relation to in-situ observations of rising-tone chorus.

2. Theory

[7] The above theories rely on particles which are Doppler-shifted to the local cyclotron frequency, that is, having parallel velocities

$$v_{||} = v_R = \frac{1}{k}\left(\omega - \frac{\Omega_e}{\gamma}\right) \tag{1}$$

where ω and k are the frequency and wave number of the whistler wave, $\Omega_e = eB_0/m$ is the gyrofrequency, B_0, c, $-e$ and m are the background magnetic field, speed of light, electron charge and rest mass, and $\gamma^2 = 1/[1 - (v_{||}^2 + v_\perp^2)/c^2]$ is the relativistic correction. These particles interact resonantly with the wave, and can gain or lose large amounts of energy; it is their dynamics which control the growth or damping of the wave.

[8] For finite-amplitude waves, some of the resonant particles can become trapped in the wave field, interacting with it over many wave periods. Trapped particles bunch about a specific phase within the wave, leading to a current which is also resonant with the wave [*Dysthe*, 1971]. The $J \times B$ force

[1]Swedish Institute of Space Physics, Uppsala, Sweden.
[2]Institute of Geophysics and Planetary Physics, University of California, Los Angeles, California, USA.
[3]Institut für Geophysik und Extraterrestrische Physik, Braunschweig, Germany.
[4]Space Sciences Laboratory, University of California, Berkeley, California, USA.
[5]Laboratoire de Physique des Plasmas, CNRS/Ecole Polytechnique/UPMC, Velizy, France.

0094-8276/11/2010GL045793

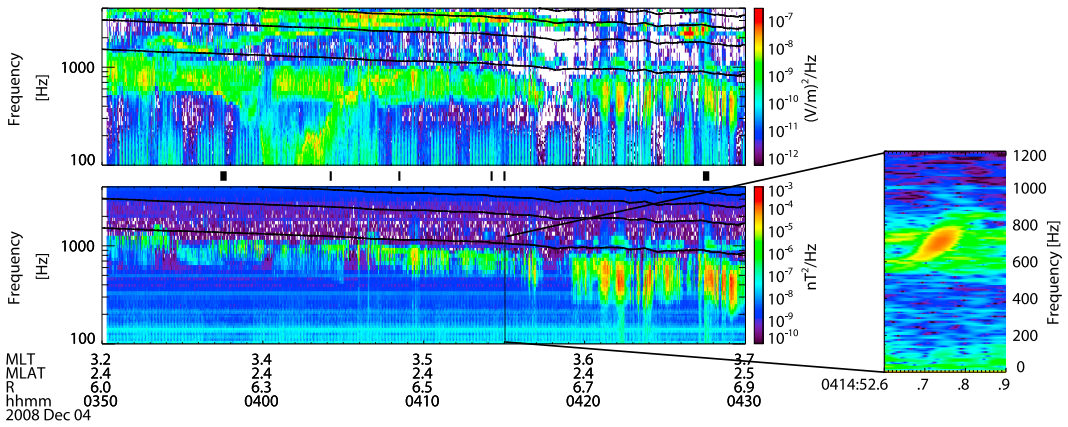

Figure 1. Spectra of (top) electric and (bottom) magnetic wave activity on THEMIS-D, with half-multiples of the local gyrofrequency in black. Black bars between the panels denote times when high-resolution timeseries data are available. The inset shows a single chorus element: 0.3 seconds of magnetic power spectra, with a linear frequency axis.

resulting from this current can then do work and transfer energy between the wave and the particles. If J_E is the current perpendicular to the wave magnetic field B_w, then the wave growth/damping is governed by

$$\frac{\partial B_w}{\partial t} + v_g \frac{\partial B_w}{\partial z} = -\frac{\mu_0 v_g}{2} J_E \tag{2}$$

(OKS08) where v_g is the group velocity of the wave propagating along z.

[9] The resonant current J_E can be calculated by separating phase space into two parts: the part occupied by trapped particles, and the part occupied by untrapped particles. The trapped particles occupy a volume C in $v_{||} - \zeta$ phase space which is locked about a phase-locking angle $\zeta = \zeta_0$; the charge contained in this resonantly-moving electron hole creates a current. The untrapped particles are assumed not to generate a substantial resonant current. The signs combine such that the wave grows if the phase space density in the trapped region is less than that of its surroundings (a "hole"). Defining the perturbation g as the phase space density of the surrounding untrapped particles minus the phase space density in the hole, the resonant current J_E is

$$J_E = -e \int_0^\infty g v_\perp^2 C \sin(\zeta_0) \mathrm{d}v_\perp. \tag{3}$$

The phase-space volume C and the phase-locking angle ζ_0 are calculated by OKS08. The latter is defined through the inhomogeneity factor S as $\sin(\zeta_0) = -S$, where

$$S = -\frac{1}{\omega_t^2 \delta^2} \left\{ \gamma \left(1 - \frac{v_R}{v_g}\right)^2 \frac{\partial \omega}{\partial t} + \left[\frac{k \gamma v_\perp^2}{2\Omega_e} - \left(1 + \frac{\delta^2}{2} \frac{\Omega_e - \gamma\omega}{\Omega_e - \omega}\right) v_R \right] \frac{\partial \Omega_e}{\partial z} \right\} \tag{4}$$

with

$$\omega_t^2 = k v_\perp \frac{e B_w}{m} \tag{5}$$

$$\delta^2 = 1 - \frac{\omega^2}{c^2 k^2}. \tag{6}$$

The phase-space volume inhabited by trapped particles is an eye-shaped region in the ζ-$v_{||}$ plane centered on $v_{||} = v_R$, $\zeta = \zeta_0$ with volume

$$C = (2e)^{3/2} \delta v_\perp^{5/2} \sqrt{\frac{B_w}{m_0 k \gamma}} \int_{\zeta_1}^{\zeta_2} \sqrt{\cos\zeta_1 - \cos\zeta + (\zeta - \zeta_1) S} \mathrm{d}\zeta \tag{7}$$

where ζ_1 and ζ_2 are the edges of the trapping region: ζ_1 is the other root of $\sin(\zeta_1) = -S$ and $\cos\zeta_2 + S\zeta_2 = \cos\zeta_1 + S\zeta_1$. For a graphical description, see Figure 1 of OKS08.

[10] The essential feature of equations (4) and (7) is that the resonant current J_E is a function of the sweep rate $\partial\omega/\partial t$ through its dependence on S. This is the key to determining the sweep rate: based on equation (2), the fastest-growing wave will be that which maximizes the resonant current J_E.

[11] All that remains is to find g, the phase space density perturbation in the hole. OKS08 assumed a ring distribution of particles with a delta function at $v_\perp = v_{\perp 0}$. This simplifies equation (3), yielding an analytic prediction for the sweep rate

$$\frac{\partial \omega}{\partial t} = 0.4 \frac{\omega_t^2 \delta^2}{\gamma} \left(1 - \frac{v_R}{v_g}\right)^{-2} \tag{8}$$

(OKS08, equation 49) where ω_t and γ are to be evaluated using $v_\perp = v_{\perp 0}$.

[12] For a more general distribution, the perturbation density $g = g(v_\perp, v_{||})$ depends on details of the trapping dynamics and cannot be so easily estimated. Fortunately, the absolute value of g is not required to calculate the sweep rate. All that we require is an estimate for the functional form.

[13] The electron hole is created by electrons in first order resonance ($v_{||} = v_R$) which are trapped in phase with the wave. For a rising tone, v_R decreases with time, and these trapped particles move to smaller $v_{||}$. If this process transports a region of low phase space density into a region of high phase space density, then the trapped region has a phase space density less than its surroundings, g is positive and the wave will grow. Hence, g depends on the initial distribution function and on how the trapped particles move in $v_\perp$.

[14] Neglecting any strictly spatial variation $\partial\Omega/\partial z$ (an assumption justified a posteriori below), then all particles

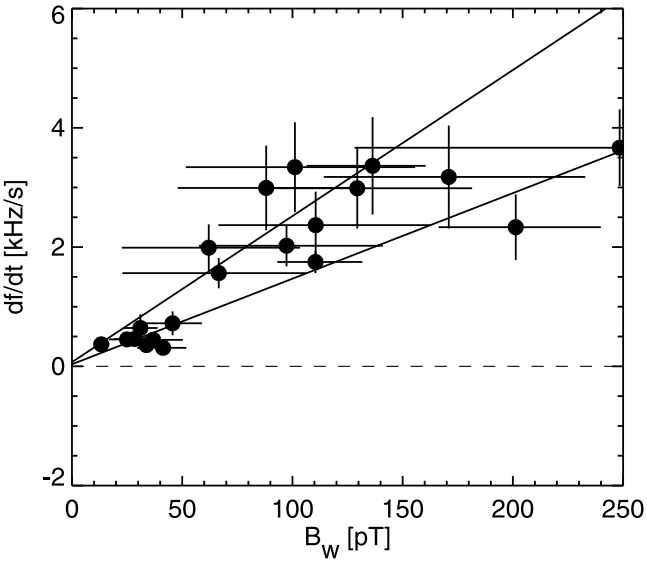

Figure 2. Sweep rate as a function of wave amplitude for the 21 identified chorus elements between 04:04 UT and 04:16. Error bars demarcate the 20th and 80th percentiles of in-sweep amplitude and from repeated estimation of $\partial f/\partial t$. Lines show the minimum and maximum predictions from the simultaneously-observed distribution functions.

near the cyclotron resonance (trapped or not) are constrained by the integral of motion

$$\left[v_{\|} + \frac{\omega}{k}\right]^2 + v_{\perp}^2 = \text{constant}. \tag{9}$$

[*Dysthe*, 1971]. The trapped electrons follow the family of curves satisfying this constraint, where ω/k always corresponds to the resonant wave. These curves are well-known from quasi-linear theory, where they go by the name of diffusion curves [*Gendrin*, 1981; *Summers et al.*, 1998].

[15] We therefore assume a functional form $g(v_{\perp},v_{||}) \propto |\Delta g_0|_R$, where $|\Delta g_0|_R$ is the change in the initial (unperturbed) phase space density g_0, evaluated along the diffusion curve R from the initial v_R to the final v_R. We assume that the unperturbed distribution is dependent only on $v_{||}$ and $v_{\perp}$. Substituting into equation (3), the resonant current becomes

$$J_E \propto -(2e)^{3/2}\delta\sqrt{\frac{B_w}{m_0 k}}\int_0^{\infty} \gamma^{-1/2} v_{\perp}^{5/2} |\Delta g_0|_R J_E^N(S) \mathrm{d}v_{\perp} \tag{10}$$

where

$$J_E^N(S) = \int_{\zeta_1}^{\zeta_2} \sqrt{\cos\zeta_1 - \cos\zeta + (\zeta - \zeta_1)S}\,\sin\zeta \mathrm{d}\zeta \tag{11}$$

is a normalized resonant current dependent only on S.

[16] We can now estimate the sweep rate directly from the observed electron distribution function. The fastest growth occurs for maximum $-J_E$. At a given B_w, we thus calculate $J_E(\partial\omega/\partial t)$ by numerically integrating equation (10),and then locate the value of $\partial\omega/\partial t$ giving the maximum $-J_E$.

[17] In some cases, the function $v_{\perp}^{5/2}|\Delta g_0|_R$ may be rather sharply peaked at some value $v_{\perp} = v_{\perp 0}$, for example if there is a steep step in the phase space density. The simplified expression (8) could then be used directly.

3. Comparison to Observations

[18] To test the predictive ability of the theory, we use data from the THEMIS mission [*Angelopoulos*, 2008], with five satellites in equatorial orbits about the Earth. The spacecraft frequently encounter chorus activity [*Li et al.*, 2010], and in Figure 1 we show time-frequency spectra of the magnetic and electric fields from THEMIS-D (P3) for an interval on 04 December 2008 when the spacecraft was at a radial distance of 6 to 7 Earth radii and within 2.5 degrees (1900 km) of the magnetic equator. The proximity to the equator places the spacecraft near the chorus source region [*Santolík et al.*, 2003] where the waves have not been significantly modified by propagation. The spectra have been computed onboard by the Digital Fields Board (DFB) [*Cully et al.*, 2008] using data from the Search Coil Magnetometer (SCM) [*Roux et al.*, 2008] and the Electric Field Instrument [*Bonnell et al.*, 2008]. Black lines in Figure 1 show 0.5, 1, 1.5 and 2 times the local gyrofrequency f_{ce} computed from the Fluxgate Magnetometer (FGM) [*Auster et al.*, 2008].

[19] The electromagnetic wave activity below $f_{ce}/2$ is consistent with lower-band chorus activity. High-resolution time-series data are available during the intervals marked between the panels of Figure 1; this data confirm that the waves are right-hand circularly polarized and field-aligned to within about 15 degrees, with rising-tone chirps. The inset shows an example of such a chirp. After 0420 UT, there is also some activity in the upper chorus band between 0.5 f_{ce} and f_{ce}, with a gap in power near 0.5 f_{ce} [*Tsurutani and Smith*, 1974]. Intense electron cyclotron harmonic waves are present near $3/2 f_{ce}$ for some of the interval.

[20] As noted by *Omura et al.* [2008], the sweep rate should be linearly related to the amplitude for constant plasma parameters (see equation (4)). Figure 2 is a plot of the observed sweep rate as a function of B_w for the 21 chorus elements identifiable in the high-resolution data intervals between 04:04 UT and 04:16 UT. The sweep rate has been estimated by plotting the spectrogram and picking out the times and frequencies of the chorus elements by hand.

[21] The broad bandwidth of the signal (see inset, Figure 1) leads to relatively large error bars in Figure 2. Nonetheless, the trend is clear: larger-amplitude elements exhibit larger sweep rates. Since the amplitude increases during the sweep, this relation may lead to slightly curved shapes in the high-resolution spectrograms (inset, Figure 1).

[22] We now focus on one particular chorus element at 04:14:52.8 UT (inset, Figure 1). Figure 3 shows a slice in the $v_{\perp} - v_{||}$ plane of the electron distribution function observed by the Electrostatic Analyzer (ESA) [*McFadden et al.*, 2008] over the 3 seconds spanning this time. The thick blue lines show the resonant ellipses (equation (1)) for whistler waves at 0.25 and 0.4 f_{ce}, corresponding to the frequency range for the chosen chorus element. Particles with energies between these blue lines can interact resonantly with the chorus element. The thick red lines are the relativistic diffusion curves [*Summers et al.*, 1998] assuming a cold dispersion relation with the observed density of 1.7 cm^{-3}. Resonant electrons are constrained to move along these curves. The dotted lines show the mirror images for $v_{||} > 0$, appropriate to particles

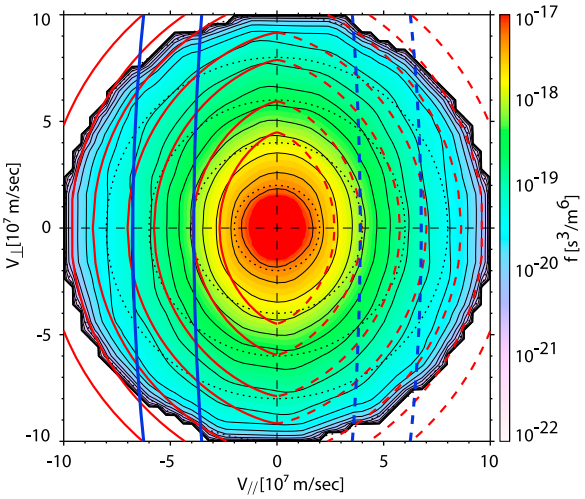

Figure 3. Electron distribution function observed between 04:14:51 UT and 04:14:54 UT. Blue solid lines show the resonant ellipses for 0.25 and 0.4 f_{ce}. Red solid lines show the diffusion curves. Resonant ellipses and diffusion curves are mirrored for $v_{||} > 0$ as dashed lines. The color table saturates at 10^{-17} s^3/m^6.

which could have resonantly interacted and then mirrored at lower altitudes.

[23] Consider the resonant interaction region between the blue lines in Figure 3. For $|v_\perp| < 6 \times 10^7$ m/s and within the resonant ellipses, the contours of constant g_0 (thin black lines) follow the diffusion curves (thick red lines), and are markedly different from isotropic (dotted lines). In contrast, g_0 is closer to isotropic outside of this region. Hence, the plasma is near the marginal stability threshold for whistler waves in the range 0.25 to 0.4 f_{ce} and whistler-stable otherwise.

[24] At perpendicular velocities above 6×10^7 m/s, the potentially-resonant part of the distribution becomes more nearly isotropic (i.e., damping). This sets an upper bound on the energy of the electrons primarily responsible for the chorus emissions. One can make a rough prediction of the sweep rate directly from this observation by assuming that the peak in $v_\perp^{5/2} |\Delta g_0|_R$ must occur near or below this value. Letting $v_{\perp 0} = 6 \times 10^7$ m/s in the simplified equation (8), we predict a sweep rate near 1.5 kHz/s at $f = 0.3\, f_{ce}$ and $B_w = 0.1$ nT. The observed sweep rate for the simultaneously-observed chorus element is (2.2 ± 0.7) kHz/s at $B_w = 0.1$ nT, which agrees surprisingly well with this very rough estimate. Strictly, the simplified equation (8) applies only if $v_\perp^{5/2} |\Delta g_0|_R$ is sharply-peaked, which is not a very good approximation here. Maximizing equation (10) numerically yields a predicted sweep rate of 1.6 kHz/s at $B_w = 0.1$ nT, in better agreement with the observed rate.

[25] We predicted the sweep rate-amplitude relation by maximizing equation (10) using the observed distribution functions and plasma parameters for the 21 elements in Figure 2. The black lines in Figure 2 show the minimum and maximum predictions. The electron distribution changes only slightly during the interval 04:04 UT to 04:16 UT, resulting in only small variations of $v_\perp^{5/2} |\Delta g_0|_R$. The change in magnetic field strength has a greater influence, resulting in faster sweep rates at earlier times. These predictions have no free parameters and use only data independent from the wave measurements. The good agreement with the wave measurements in Figure 2 provides strong experimental evidence for the nonlinear theories.

[26] The non-zero intercept of the theoretical line with $B_w = 0$ results from the spatial derivative $\partial\Omega_e/\partial z$, which we calculated assuming a dipolar field. Its small value implies that the temporal inhomogeneity dominates over the spatial inhomogeneity for a well-developed chorus element and justifies the assumption near equation (9). The spatial inhomogeneity term remains small (intercept <0.3 kHz/s) for $\partial\Omega_e/\partial z$ calculated within about 5000 km of the actual position. This is consistent with the observed size of the generation region: several thousand km [*Santolík et al.*, 2003].

4. Conclusions

[27] Theoretically, the nonlinear cyclotron-resonant theory of chorus generation is very well developed [*Dysthe*, 1971; *Nunn*, 1974; *Omura et al.*, 1991; *Trakhtengerts*, 1999]. Unfortunately, testing this theory by comparing it to experimental data is difficult, and has often involved sophisticated numerical simulation [*Nunn et al.*, 2009; *Katoh and Omura*, 2007]. However, there are a couple of new and non-trivial predictions that are more amenable to testing.

[28] First, the sweep rate is predicted to be a function of the amplitude (OKS08). As seen in Figure 2, this prediction is borne out in the THEMIS data. Much of the variation in observed chorus sweep rates can be attributed to varying amplitudes.

[29] Second, the sweep rate-amplitude relationship can be predicted based solely on the observed electron distribution function and the magnetic field strength. These predictions also agree well with the observations.

[30] While rising-tone chorus elements are observed frequently, they are not the only voice in the magnetospheric chorus. Falling tones, featureless banded emissions and obliquely-propagating waves all lie outside of the framework presented here. But for the prototypical rising-tone parallel chorus element, the good agreement between these predictions and the independently-observed sweep rates provides strong evidence in support of the cyclotron-resonant trapping theory of chorus generation as expressed by *Omura et al.* [2008].

[31] **Acknowledgments.** We acknowledge NASA contract NAS5-02099 for the use of data, and J.P. McFadden for the use of ESA data. The research of CMC was funded by the Swedish Research Council, grant 2009-3957.

References

Angelopoulos, V. (2008), The THEMIS mission, *Space Sci. Rev.*, *141*(1–4), 5–34, doi:10.1007/s11214-008-9336-1.

Auster, H., et al. (2008), The THEMIS fluxgate magnetometer, *Space Sci. Rev.*, *141*(1–4), 235–264, doi:10.1007/s11214-008-9365-9.

Bonnell, J., F. Mozer, G. Delory, A. Hull, R. Ergun, C. Cully, V. Angelopoulos, and P. Harvey (2008), The electric field experiment on the THEMIS satellites, *Space Sci. Rev.*, *141*(1–4), 303–341, doi:10.1007/s11214-008-9469-2.

Cully, C. M., R. E. Ergun, K. Stevens, A. Nammari, and J. Westfall (2008), The THEMIS Digital Fields Board, *Space Sci. Rev.*, *141*(1–4), 343–355, doi:10.1007/s11214-008-9417-1.

Dysthe, K. B. (1971), Some studies of triggered whistler emissions, *J. Geophys. Res.*, *76*(28), 6915–6931, doi:10.1029/JA076i028p06915.

Gendrin, R. (1981), General relationships between wave amplification and particle diffusion in a magnetoplasma, *Rev. Geophys.*, *19*(1), 171–184, doi:10.1029/RG019i001p00171.

Helliwell, R. A. (1965), *Whistlers and Related Ionospheric Phenomena*, Stanford Univ. Press, Stanford, Calif.

Katoh, Y., and Y. Omura (2007), Computer simulation of chorus wave generation in the Earth's inner magnetosphere, *Geophys. Res. Lett.*, *34*, L03102, doi:10.1029/2006GL028594.

Kennel, C. F., and H. E. Petschek (1966), Limit on stably trapped particle fluxes, *J. Geophys. Res.*, *71*(1), 1–28, doi:10.1029/JZ071i001p00001.

Li, W., et al. (2010), THEMIS analysis of observed equatorial electron distributions responsible for the chorus excitation, *J. Geophys. Res.*, *115*, A00F11, doi:10.1029/2009JA014845.

McFadden, J. P., C. W. Carlson, D. Larson, M. Ludlam, R. Abiad, B. Elliott, P. Turin, M. Marckwordt, and V. Angelopoulos (2008), The THEMIS ESA plasma instrument and in-flight calibration, *Space Sci. Rev.*, *141*(1–4), 277–302, doi:10.1007/s11214-008-9440-2.

Nunn, D. (1974), A self-consistent theory of triggered VLF emissions, *Planet. Space Sci.*, *22*(3), 349–378, doi:10.1016/0032-0633(74)90070-1.

Nunn, D., O. Santolik, M. Rycroft, and V. Trakhtengerts (2009), On the numerical modelling of VLF chorus dynamical spectra, *Ann. Geophys.*, *27*(6), 2341–2359, doi:10.5194/angeo-27-2341-2009.

Omura, Y., D. Nunn, H. Matsumoto, and M. Rycroft (1991), A review of observational, theoretical and numerical studies of VLF triggered emissions, *J. Atmos. Terr. Phys.*, *53*(5), 351–358, doi:10.1016/0021-9169(91)90031-2.

Omura, Y., Y. Katoh, and D. Summers (2008), Theory and simulation of the generation of whistler-mode chorus, *J. Geophys. Res.*, *113*, A04223, doi:10.1029/2007JA012622.

Roux, A., O. Le Contel, C. Coillot, A. Boubdellah, B. de la Porte, D. Alison, S. Ruocco, and M. C. Vassal (2008), The Search Coil Magnetometer for THEMIS, *Space Sci. Rev.*, *141*(1–4), 265–275, doi:10.1007/s11214-008-9455-8.

Santolík, O. (2008), New results of investigations of whistler-mode chorus emissions, *Nonlinear Processes Geophys.*, *15*, 621–630, doi:10.5194/npg-15-621-2008.

Santolík, O., D. A. Gurnett, J. S. Pickett, M. Parrot, and N. Cornilleau-Wehrlin (2003), Spatio-temporal structure of storm-time chorus, *J. Geophys. Res.*, *108*(A7), 1278, doi:10.1029/2002JA009791.

Santolík, O., D. A. Gurnett, J. S. Pickett, M. Parrot, and N. Cornilleau-Wehrlin (2004), A microscopic and nanoscopic view of storm-time chorus on 31 March 2001, *Geophys. Res. Lett.*, *31*, L02801, doi:10.1029/2003GL018757.

Santolík, O., E. Macusova, E. E. Titova, B. V. Kozelov, D. A. Gurnett, J. S. Pickett, V. Y. Trakhtengerts, and A. G. Demekhov (2008), Frequencies of wave packets of whistler-mode chorus inside its source region: A case study, *Ann. Geophys.*, *26*, 1665–1670, doi:10.5194/angeo-26-1665-2008.

Summers, D., R. M. Thorne, and F. Xiao (1998), Relativistic theory of wave-particle resonant diffusion with application to electron acceleration in the magnetosphere, *J. Geophys. Res.*, *103*(A9), 20,487–20,500, doi:10.1029/98JA01740.

Trakhtengerts, V. (1999), A generation mechanism for chorus emission, *Ann. Geophys.*, *17*(1), 95–100, doi:10.1007/s00585-999-0095-4.

Trakhtengerts, V. Y., A. G. Demekhov, E. E. Titova, B. V. Kozelov, O. Santolik, E. Macusova, D. Gurnett, J. S. Pickett, M. J. Rycroft, and D. Nunn (2007), Formation of VLF chorus frequency spectrum: Cluster data and comparison with the backward wave oscillator model, *Geophys. Res. Lett.*, *34*, L02104, doi:10.1029/2006GL027953.

Tsurutani, B. T., and E. Smith (1974), Postmidnight chorus: A substorm phenomenon, *J. Geophys. Res.*, *79*(1), 118–127.

Tsurutani, B. T., E. Smith, J. H.I. West, and R. Buck (1979), Chorus, enegetic electrons and magnetospheric substorms, in *Wave Instabilities in Space Plasma*, edited by P. Palmadesso and K. Papadopoulos, pp. 55–62, D. Reidel, Dordrecht, Netherlands.

V. Angelopoulos, Institute of Geophysics and Planetary Physics, University of California, Los Angeles, CA 90095, USA.

U. Auster, Institut für Geophysik und Extraterrestrische Physik, Mendelssohnstrasse 3, D-38106 Braunschweig, Germany.

J. Bonnell, Space Sciences Laboratory, University of California, Berkeley, CA 94720, USA.

C. M. Cully, Swedish Institute of Space Physics, Box 537, SE-75121 Uppsala, Sweden. (chris@irfu.se)

O. Le Contel, Laboratoire de Physique des Plasmas, CNRS/Ecole Polytechnique/UPMC, 10-12 Ave. de l'Europe, F-78140 Velizy CEDEX, France.